Digest Journal of Nanomaterials and Biostructures Vol. 11, No. 2, April - June 2016, p. 425 - 434

NOVEL SUPER ADSORBENTS (PVA AND PVA/Cu-MOF NANOFIBRES) AS EFFECTIVE LEAD IONS REMOVER IN AQUEOUS SOLUTION

N. D. SHOOTO[a*], D. WANKASI[a], L. SIKHWIVHILU[b], E. D. DIKIO[a], F. MTUNZI[a], M. S. MAUBANE[c]

[a]*Applied Chemistry and Nano-Science Laboratory, Department of Chemistry, Vaal University of Technology P.O. Box X021, Vanderbijlpark 1900, South Africa*

[b]*Advanced Materials Division, Mintek, Nanotechnology Innovation Centre, Private Bag X3015, Randburg 2125, South Africa*

[c]*Microscopy and Microanalysis Unit, University of the Witwatersrand, Wits, 2050, South Africa*

In this study electrospun PVA nanofibres were functionalized with Cu-MOFs to produce a novel super adsorbing material. The novel nano-composite was analysed by scanning electron microscope (SEM), Fourier transform infrared (FTIR) and Thermogravimetric analysis (TGA). SEM micrograms showed that uniform and non-beaded nanofibres were fabricated. TGA plots showed PVA/Cu-MOF nanofibres exhibit higher decomposition temperature than PVA nanofibres. Thus, it confirmed the interactive force between PVA nanofibres and Cu-MOF. FTIR spectra also exhibited shifts in critical functional groups positions thus it confirmed that there was a given amount of Cu-MOF embedded in the electrospun fibrous mat. Sorption studies were executed to analyse the adsorption of lead ions in aqueous solution. Factors influencing adsorption of lead ions onto PVA nanofibres and functionalized PVA nanofibres (PVA/Cu-MOF) such as concentration, contact time and temperature effect were examined. The thermodynamic parameters: apparent enthalpy (ΔH^o) and entropy (ΔS^o) showed that the adsorption of lead ions onto the electrospun nanofibres was spontaneous and exothermic respectively.

(Received February 22, 2016; Accepted April 20, 2016)

Keywords: Adsorption, nanofibres, electrospinning, polymer

1. Introduction

Water-waste contaminated by heavy metals is very toxic to humans and to the aquatic environment [1]. Unlike organic pollutants, heavy metals such as lead Pb(II) and chromium Cr(VI) are not biodegradable and easily removed from aqueous solution; hence their concentrations should be reduced to acceptable levels before disposal into the environment [2]. These toxic metals enter human body mainly via inhalation, ingestion and skin. Pb(II) causes many illness and disorders depending on degree and duration of exposure. Lead generally interferes metabolism processes and is an enzyme inhibitor [3]. Toxic effects of lead are impaired fitness and reproduction. It can also damage the central nervous system and other main organs such as kidney, liver and heart and hinders human cell processes [4].

Many technologies have been developed and employed for the removal of lead from aqueous solution. That include ion exchange, adsorption, photocatalysis, floatation, hyper-filtration, chemical precipitation and reverse osmosis [5]. Among these methods adsorption is the procedure of choice because it is cheap, effective, low energy cost, environmental friendliness and several heavy metals can be removed simultaneously [6-7]. Many materials have been studied as potential lead ion adsorbents; reported materials include polymers like polystyrene and polymethylmethacrylate [8], biomass like coconut shell and palm kernel shell [9] and metal organic frameworks such as cobalt-MOFs [10-11], copper-MOFs [12].

[*]Corresponding author: davidshooto12@gmail.com

Polymeric nanofibres have unique physical and chemical properties which in turn have many potential uses in electronic devices, super capacitors, rechargeable batteries, sensors [13-14]. Most importantly, their heavy metal remover ability has made them to be great candidate adsorbent materials. Many polymeric nanofibres have been used for the treatment of polluted waste waters, modified nanofibres such as polyaniline (PANI) [15], polypyrrole (PPy) [16], poly(m-phenylenediamine) (PmPD) [17], poly(o-phenylenediamine) (PoPD) [18] and p-phenylenediamine (pPD) [19] has been reported to have good adsorption performance toward lead Pb(II), copper Cu(II), chromium Cr(VI), silver Ag(I), mercury Hg(II) and arsenic As(V). Surface modification of nanofibres leads to larger adsorption capacity. Thus, it is important to prepare adsorbents with a large surface area to maximize adsorption [20]

This has led to the exploration for adsorbent materials with high affinity for lead ions in aqueous solution. In this study, we have reported the synthesis of polyvinyl alcohol (PVA) nanofibres and PVA nanofibres functionalized with copper metal organic frameworks (Cu-MOFs) (PVA/Cu-MOFs) by electrospinning. We also report their adsorption properties of lead ions in aqueous solution.

2. Experimental

Materials

Polyvinyl alcohol [$(CH_2CH(OH))_n$, PVA, fully hydrolysed, Sigma-Aldrich], *N*,*N*-Dimethylformamide [$HCON(CH_3)_2$, DMF, 99.8%; AnalaR], Copper(II)nitrate trihydrate [$Cu(NO_3)_2.3H_2O$, 99%, Sigma-Aldrich], 1,2,4,5-Tetrabenzenecarboxylic acid [$C_6H_2(CO_2H)_4$, 96%, Sigma-Aldrich], Methanol [CH_3OH, 99.9%; Sigma-Aldrich].

All the reagents were obtained from commercial sources and were used without further purification.

Sample preparation

Preparation of Cu-MOF

The Cu-MOF was synthesized by solvothermal method. 80 ml DMF was transferred into a round bottom flask, Subsequently (0.012 mol) $Cu(NO_3)_2$ and (0.012 mol) 1,2,4,5-tetrabenzenecarboxylic acid were dissolved in DMF by mild stirring. The solution was refluxed for 2 hours at 120^{o}C while stirring. Blue crystals were obtained and isolated by centrifuge and washed with methanol to remove excess DMF. The obtained crystals were then dried in oven at 40 ^{o}C for 30 minutes and used for further experiments.

Preparation for electrospinning

PVA solution was prepared by dissolving (2.7 g) PVA into hot distilled water (27.3 g). The polymer solution (10 ml) was mixed with (0.01 g) Cu-MOF powder for 1 hour on a magnetic stirrer. The polymer solution mixture was transferred into a 20 ml syringe. The experimental set-up used consisted of a high voltage power supply, syringe and a collector (aluminium foil). A positive terminal high voltage of 15kV was applied at a syringe needle to charge the polymer solution. The electrospun nanofibres were accumulated on aluminium foil connected to electrically grounded metal plate, 15 cm apart from the syringe needle. Electrospinning process was operated at ambient environment.

Lead solution preparation

Pb^{2+} stock solution (100 ppm) was prepared by dissolving 0,1 g $Pb(NO_3)_2$ in 1 L of distilled water. Dilutions were made to 80, 60, 40 and 20 ppm respectively.

Adsorption procedure

Concentration effect

0.1g of the nano-composite (PVA/Cu-MOF) nanofibres mat was weighed, and placed into each of the 5 test tubes. 20ml of metal ion solution with standard concentration of 20, 40, 60, 80 and 100 ppm from $Pb(NO_3)_2$ solutions were transferred to each beaker containing the weighed

nano-composite. It was agitated on a shaker for 30 min the remaining nanofibres suspension was removed by centrifugation and decanted. The remaining solutions were stored for lead ion (Pb^{2+}) analysis using atomic adsorption spectrometer.

Time dependence studies

0.1g of the nano-composite (PVA/Cu-MOF) nanofibres mat was weighed and transferred into each of the 3 test tubes. 20ml of the metal ion solution with standard concentration of 60 ppm from $Pb(NO_3)_2$ solution was transferred to each beaker containing the weighed nano-composite. It was agitated on a shaker for each time intervals of 10, 30 and 60 min respectively. The nanofibres suspension were centrifuged and decanted. The remaining solutions were stored for lead ion (Pb^{2+}) analysis.

Temperature effect

0.1g of the nano-composite (PVA/Cu-MOF) nanofibres mat was weighed placed in 4 test tubes. 20ml of the metal ion solution with standard concentration of 60 ppm from $Pb(NO)_3)_2$ was transferred to beaker containing the weighed nano-composite. It was agitated 30 min at temperatures of 25, 40, 60 and 80 ^oC respectively using water bath. The solution with nanofibres suspension was centrifuged and decanted. The remaining solutions were stored for lead ion (Pb^{2+}) analysis.

Same procedure as mentioned above for concentration, time and temperature effect was followed to evaluate Pb^{2+} ability to be adsorbed by PVA nanofibres mat

Characterization

The chemical features of the as-prepared electrospun nanofibres were examined by SEM, FTIR and TGA. The surface morphology measurements were recorded with a JOEL 7500F Emission scanning electron microscope. Thermogravimetric Analyzer (TGA), Perkin Elmer TGA 4000 was used, analyses were performed from 30 to 900^oC at a heating rate of 10^oC/min under a nitrogen atmosphere. Fourier transformed infrared spectroscopy (FTIR), Perkin Elmer FT-IR/FT-NIR spectrometer, spectrum 400. The measuring range extended from 4000 to 520 cm^{-1}. After adsorption, Atomic Absorption Spectroscopy (AAS) Shimadzu ASC 7000 auto sampler was used to measure the remaining Pb^{2+} ions in the solution.

Data Analysis

The sorbed amount of lead ions onto the adsorbent was determined using the following equation for batch dynamic studies:

$$q_e = \frac{V}{M}(C_O - C_e) \quad (1)$$

where
q_e: Pb(II) concentration sorbed onto nano-composite at equilibria point (mg of metal ion/g of adsorbent).
C_o: Initial concentration of Pb(II) in solution (in ppm).
C_e: Equilibriua point concentration of Pb(II) in solution (in ppm).
V: Initial volume of Pb(II) solution used (in L).
M: Weight of the nano-composite.

Langmuir graphs were plotted by applying the following equation

$$\frac{m}{x} = \frac{1}{abC_e} + \frac{1}{b} \quad (2)$$

where
x: Pb(II) sorbed per mass of nano-composite (in mg/L)
a and b: are the Langmuir constants obtained from the slope and intercepts of the plots.

Langmuir isotherm was showed in terms of an equation of separation factor (S_f). It determines a type of adsorption isotherm. When (S_f) is greater than 1, the isotherm is unfavourable; if (S_f) is 1 (linear), if 0 < (S_f) < 1.0 (favourable), and (S_f) = 0 (irreversible).

$$S_f = \frac{1}{1+ aC_o} \tag{3}$$

The degree of surface coverage of adsorbent covered by lead ions was calculated using

$$\theta = 1 - \frac{C_e}{C_o} \tag{4}$$

The capability of nanofibres to reduce the amount of Pb(II) in solution was evaluated by total cycles of equilibrium adsorption needed according to the value of the partition coefficient (K_d) in equation 5

$$K_d = \frac{C_{ads}}{C_{aq}} \tag{5}$$

where
C_{aq}: Concentration of Pb(II) in solution, (in mg/L)
C_{ads}: Concentration of Pb(II) in nano-composite (in mg/L)

Suzuki equation was used to determine the heat of adsorption (Q_{ads}) as expressed in the below equation

$$In\ \theta = \frac{InK_O C_O}{T^{0.5}} + \frac{Q_{ads}}{RT} \tag{6}$$

where
T: Temperature of the solution (in K)
K_o: Constant
R: Gas constant (8.314 J/Kmol).

Linearized Arrhenius equation was used to the obtained data to determine the activation energy (E_a) and sticking probability $S*$.

$$In(1 - \theta) = S^* + \frac{E_a}{RT} \tag{7}$$

Gibbs free energy (ΔG^o) of the sorption process was applied to evaluate the spontaneity.

$$\Delta G^\circ = RTInK_d \tag{8}$$

Further investigation was done to measure the enthalpy (ΔH°) and entropy (S°) of the sorption process by using equation 9.

$$\Delta G^\circ = \Delta H^\circ - T\Delta S^\circ \tag{9}$$

The number of hopping (n) was calculated by relating it to the surface coverage (θ).

$$n = \frac{1}{(1-\theta)\theta} \tag{10}$$

Other thermodynamic parameters such as adsorption potential (A) were tested by applying

$$A = -RT\ In\frac{C_o}{C_e} \tag{11}$$

3. Results and discussion

The SEM micrographs of electrospun PVA nanofibres are presented in figure 1 (a), (b) and for electrospun PVA/Cu-MOF nanofibres is figure 1 (c), (d). It was observed that very uniform and non-beaded nanofibres were fabricated for PVA nanofibres as presented in figure 1 (a) and (b). The functionalised PVA/Cu-MOF nanofibres in figure 1 (c) and (d) showed the formation of patches in some regions which led to partial cross linkage and network structures hence it reduces the frailness of nanofibres. Slight detects were also observed on the PVA/Cu-MOF nanofibres as highlighted on the figure 1 (c) and (d), this could be due to the presence of Cu-MOF embedded in the nanofibres. Other than that no other morphological changes was observed in the view of the SEM images.

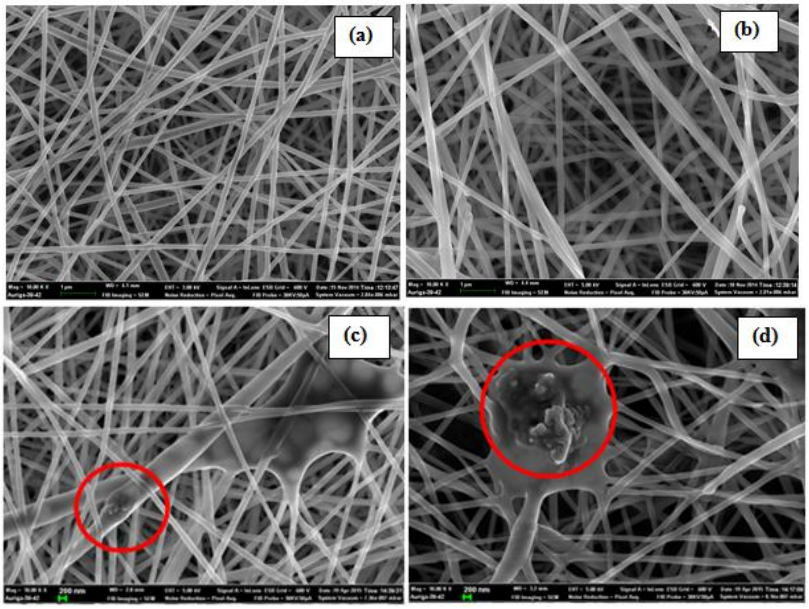

Fig. 1 (a) and (b) SEM micrographs of PVA nanofibres. ***(c)*** *and* ***(d)*** *micrographs of PVA/Cu-MOF nanofibres.*

TGA was used to study the thermal stability of the as-prepared electrospun PVA nanofibres and PVA/Cu-MOF nanofibres. TGA-DTA curves in figure 2 (a) PVA nanofibres and (b) PVA/Cu-MOF nanofibres. In figure 2 (a) it was observed that the nano-composite undergoes multiple decomposition stages: first decomposition occurred between 30 – 75 ^{o}C which was mainly caused by the loss of water molecules that was physisorbed [22]. Second decomposition occurred between 149 – 371 ^{o}C of which this is the most intense weight loss it corresponds to the side chains of PVA, the loss of H-bond between PVA molecules and O-bond between C-O. Third decomposition 378 – 489 ^{o}C corresponds to the disintegration of the main chain of PVA [23]. PVA/Cu-MOF nanofibres figure 2 (b) it was observed that it only undergoes two decomposition steps. First decomposition occurred between 30 – 91 ^{o}C, second decomposition 150 – 501 ^{o}C. PVA/Cu-MOF nanofibres exhibit higher decomposition temperature than PVA nanofibres. Thus, it confirmed the interactive force between Cu-MOF and PVA nanofibres.

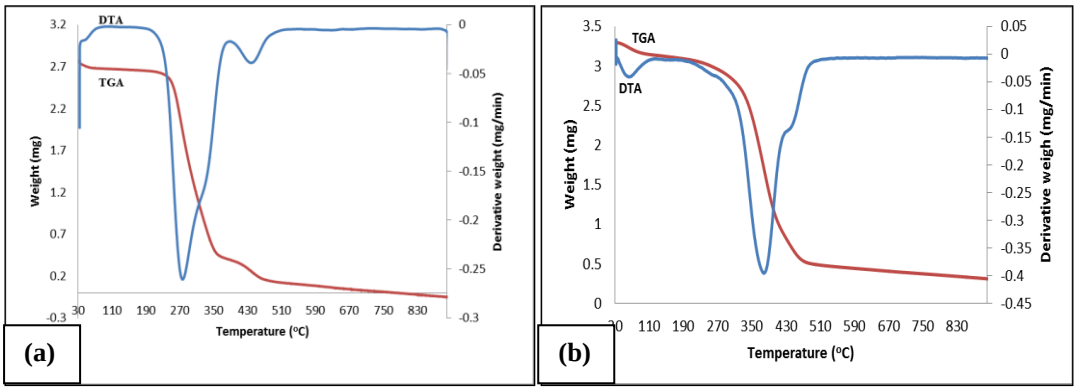

Fig. 2 Thermalgravimetric analysis (TGA) and Derivative thermogravimetric analysis (DTA) of (a) PVA nanofibres and (b) PVA/Cu-MOF nanofibres

In order to examine whether Cu-MOF was incorporated to the electrospun PVA nanofibres, FTIR spectra of both electrospun PVA and PVA/Cu-MOF nanofibres were measured to monitor changes in the IR spectra as shown in figure 3. On the spectra of electrospun PVA nanofibres mat, the major peaks observed were as follows: bands at 3293.85 and 1660.20 cm^{-1} are assigned to the stretching and bending vibrations of (O-H) respectively, two vibration bands at 2936.50 and 2911.11 cm^{-1} are assigned to (C-H), a sharp band at 1100.27 is attributed to the vibration of (C-C), a medium shoulder peak at 917.30 cm^{-1} is linked to the vibration of (C-O). By comparing the spectra of electrospun PVA and PVA/Cu-MOF nanofibres, several shifts in peaks were observed. As highlighted on the spectra. It is concluded that there were a given amount of Cu-MOF in electrospun fibrous mat.

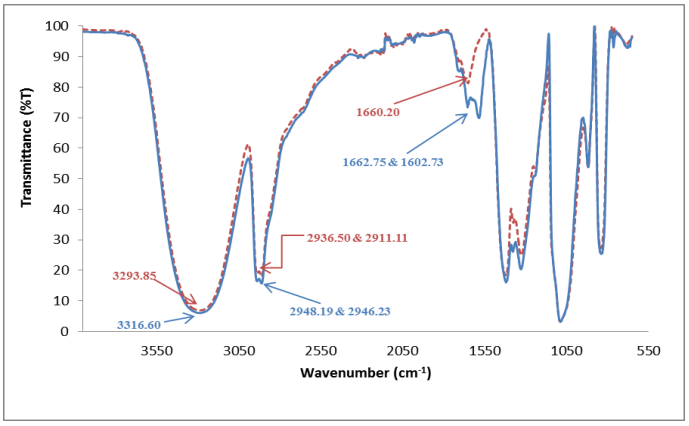

Fig. 3 FTIR spectra of PVA nanofibres (red dotted line) and PVA/Cu-MOF nanofibres (blue solid line)

The effect of temperature on Pb(II) sorption onto PVA nanofibres and PVA/Cu-MOF nanofibres was investigated at different temperatures of 25, 40, 60 and 80 ^{o}C as shown in figure 4. In both instances adsorption rate was rapid from 0-25 ^{o}C, after which as temperature increased there was no improvement observed in adsorption rate as equilibrium was reached. These results showed that temperature has no significant impact on the sorption of Pb(II) onto nanofibres composites.

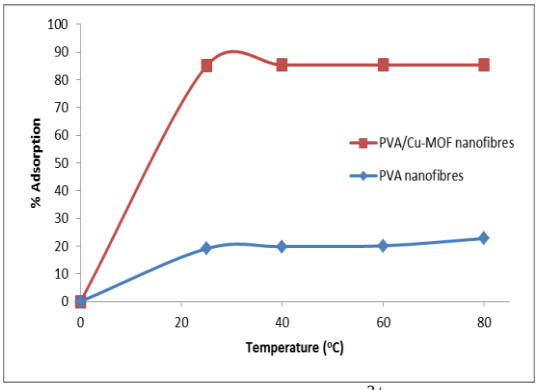

Fig. 4 Temperature effect on adsorption of Pb^{2+} ions onto PVA nanofibres (-♦-) and PVA/Cu-MOF nanofibres (-■-)

Time effect indicates the duration required for maximum sorption to occur. Figure 5 shows the effect of time at (10, 30 and 60 min) on the sorption of Pb(II) ions onto electrospun nanofibres. It was observed that Pb(II) sorption onto PVA nanofibres and PVA/Cu-MOF nanofibres was very rapid at the initial stages especially first 10 minutes of the contact period. This is because of the presence of multiple vacant sites at the beginning of the sorption process but proportionally as the sorption sites decreased in number and became saturated, the sorption rate was slowed down until equilibrium was reached. Maximum percentage sorption of 10.25% and 92.74% occurred at 60 min for PVA and PVA/Cu-MOF nanofibres respectively. Nanofibres surface vacant sites were filled relatively fast this suggests that Pb(II) uptake was rapid and after which the unreacted vacant sites were hard to be reached due to repulsive forces between Pb(II) ions. Results showed that the modified electrospun nanofibres adsorbed far much better than the unmodified nanofibres.

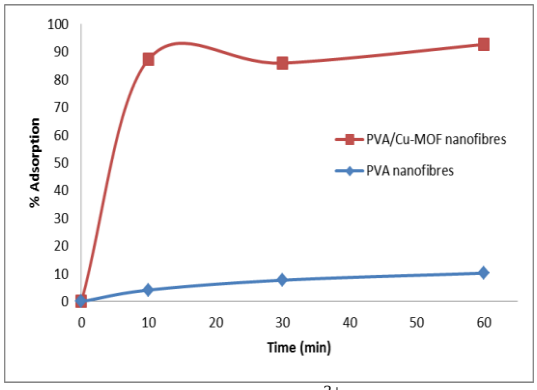

Fig. 5 Time effect on adsorption of Pb^{2+} ions onto PVA nanofibres (-♦-) and PVA/Cu-MOF nanofibres (-■-)

The percentage sorption of Pb(II) by PVA and PVA/Cu-MOF nanofibres at different concentrations of Pb(II) (20, 40 and 60, 80 and 100 ppm) is presented in figure 6. It was observed that as the concentration increased the adsorption also increased until it reached equilibrium. This is because at lower concentration more pore spaces were available for the Pb(II) but as the concentration further increased, the adsorption capacity of the nanofibres decreased due to reduced availability of free pore spaces and active sites.

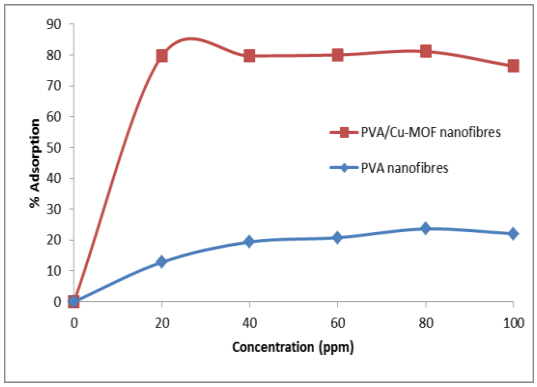

Fig. 6 Concentration effect on adsorption of Pb^{2+} ions onto PVA nanofibres (-♦-) and PVA/Cu-MOF nanofibres (-■-)

The surface covered by Pb(II) ions is given as 0.2206 and 0.7636 for PVA and PVA/Co-MOF nanofibres respectively as shown in table 1. This suggested that over 22 and 76 % of the surfaces of PVA and PVA/Cu-MOF nanofibres were covered by the Pb(II) ions. Further-more it indicated that higher degree of adsorption occurred on PVA/Cu-MOF nanofibres (76 %) as compared to PVA electrospun nanofibres (22%).

To determine whether Pb(II) to electrospun nanofibres sorption were favourable or not, separation factor (S_f) was calculated. (S_f) values were 0.7028 and 0.4112 for PVA and PVA/Cu-MOF nanofibres respectively. Both (S_f) values were below one and more than zero which indicated that the sorption of Pb(II) ions onto the electrospun composites was favourable as presented in table 1.

The capability of the electrospun nanofibre composites to reduce the amount of lead ions in solution was determined by cycles of equilibria sorption process required according to the value of the partition coefficient (K_d) as presented in table 1. The value of (3.5315) for PVA and (0.3095) for PVA/Cu-MOF nanofibres. This suggests that PVA/Cu-MOF nanofibres is a more effective adsorbent as the required cycles of equilibria sorption are fewer to reduce the levels of Pb(II) ions in aqueous solution

Adsorption capacity of the electrospun nano-composites were calculated to be 25.50 and 94.86 for PVA and PVA/Cu-MOF nanofibres respectively using equation 1. This indicated that more Pb(II) ions up-take occurred on PVA/Cu-MOF nanofibres.

Table 1. Equilibrium and kinetic parameters

Composite	Surface coverage (θ)	Separation factor (S_f)	Sorption coefficient (K_d)	Adsorption capacity (mol/g)
PVA nanofibres	0.2206	0.7028	3.5315	25.50
PVA/Cu-MOF nanofibres	0.7636	0.4112	0.3095	94.86

The heat of adsorption (Q_{ads}) for the sorption of Pb(II) ions was calculated and obtained the values of (-5.3145) and (-0.5653) respectively for PVA and PVA/Cu-MOF nanofibres. Negative values indicated that the sorption that occurred was exothermic. Pb(II) to electrospun nanofibres sorption favoured more of low temperatures. Thus increased temperatures did not improve the sorption processes.

Activation energy (E_a) and sticking probabilities (S*) were determined by using equation 7. The values of (E_a) and (S*) are respectively presented in table 2 as (-2.1584) and (0.7734) for PVA nanofibres, (-16.0568) and (0.8026) for PVA/Cu-MOF nanofibres. On both instances

relativity low and negative (E_a) values indicated that very low energy was required to start the sorption and that the sorption processes were exothermic. The sticking probability (S*) measures the ability of an Pb(II) to stay attached onto nanofibres. If S* > 1 (no sorption), S* = 1 (mixture of physisorption and chemisorption), S* = 0 (bound, chemisorption), 0 < S* < 1 (bound, physisorption). The obtained S* values for the sorption of Pb(II) ions onto electrospun nanofibres were less than one which indicated the sorption was favourable and physisorption mechanism was dominant

The Gibbs free energy (ΔG^o) was determined to assess the spontaneousness of the sorption process. Obtained (ΔG^o) values of (-3.592) for PVA nanofibres and (-5.167) for PVA/Cu-MOF nanofibres, were in the negative region indicated that the sorption were spontaneous, no extra energy was required to kick start the process.

The apparent enthalpy (ΔH^o) and entropy (ΔS^o) of adsorption were also calculated as shown in table 2. The values of enthalpy change (ΔH^o) were (-2.6857) and (-0.3788) for PVA and PVA/Cu-MOF nanofibres respectively. Negative values for (ΔH^o) suggested that the sorption favoured lower temperatures. The entropy change (ΔS^o) gave positive values (2.9) and (15.7) for PVA and PVA/Cu-MOF nanofibres respectively, this indicated that Pb(II) ions were not restricted in the electrospun nanofibres and physisorption mechanism was dominant.

The probability of Pb(II) in finding vacant site on the surface of electrospun nanofibres was determined by the number of hopping (n). PVA and PVA/Cu-MOF nanofibres respectively gave the (n) values of (1) and (8). Faster sorption is indicated by a lower hopping number. Lower number of hopping (n) values for both PVA and PVA/Cu-MOF nanofibres showed that the sorption of Pb(II) ions was very rapid.

The apparent changes in chemical potential that occurred as Pb(II) ions moved from solution to the surface of electrospun nanofibres were calculated to be (0.7566) for PVA nanofibres and (-5.6328) for PVA/Cu-MOF nanofibres.

Table 2. Thermodynamic parameters

Composite	Heat of adsorption, Q_{ads} (KJ/mol.K)	Sticking probability (S*)	Activation energy, Ea (JK.mol)	Gibbs free energy of adsorption, ΔG^o (KJ/mol)	Apparent entropy, ΔS^o (J/mol.K)	Apparent enthalpy, ΔH^o (J/mol)	Hopping number, n	Adsorption potential, A (KJ/mol)
PVA nanofibers	-5.3145	0.7734	-2.1584	-3.592	2.9	-2.6857	1	0.7566
PVA/Cu-MOF nanofibers	-0.5653	0.8026	-16.0568	-5.167	15.7	-0.3788	8	-5.6328

4. Conclusion

Novel PVA/Cu-MOF electrospun nanofibres was successfully fabricated and used as an adsorbent for Pb(II) in aqueous solution. Kinetics studies showed that the uptake of Pb(II) ions by the nanofibres was very rapid, favoured at low temperatures and predominated by physisorption mechanism. Novel PVA/Cu-MOF electrospun nanofibres possesses unique properties such as network and partial cross-linked structure so it adsorbed and trapped metal ions more efficiently

Acknowledgements

This work was supported by a research grant from the Faculty of Applied and Computer Science Research and Publications Committee of Vaal University of Technology. National research fund is greatly acknowledged

References

[1] G. Pandey, S. Madhuri, Res. J. Animal, Veterinary and Fishery Sci **2**, 17 (2014).
[2] M. A. P. Cechinel, S. M. A. Souza, A.A. Souza, J. Clean. Prod **65**, 342 (2014).
[3] N. Bensacia, I. Fechete, S. Moulay, O. Hulea, A. Boos, F. Garin, C. R. Chimie **17**, 869 (2014).
[4] M. Praveena, V. Sandeep, N. Kavitha, K. R. Jayantha, Res. J. Animal, Veterinary and Fishery Sci **1**, 1 (2013).
[5] N. Tewari, P. Vasudevan, B. K. Guha, Bioch. Eng. J **23**, 185 (2005).
[6] M. T. Yagub, T. K. Sen, S. Afroze, H.M. Ang, Adv. Colloid Interface Sci **209**, 172 (2014).
[7] X. Li, S. Chen, X. Fan, X. Quan, F. Tan, Y. Zhang, J. Gao, J. Colloid Interface Sci **447**, 120 (2015).
[8] D. Wankasi, E. D. Dikio, Asian J. Chem **24**, 8295 (2014).
[9] D. Wankasi, E. D Dikio, Asian J. Chem **2**, 690 (2015).
[10] N. D. Shooto, N. Ayawei, D. Wankasi, L. Sikhwivhilu, E. D. Dikio, Asian J. Chem **28**, 277 (2016).
[11] E. D. Dikio, N. D. Shooto, Patent J. **49**, 3 (2016). (Provisional patent 2016/01816)
[12] M. Afshin, H. Bagher, N. Maryam, W. J. Sang, J. Ind. Eng. Chem **28**, 211 (2015).
[13] S.I. Cho, S.B. Lee, Acc. Chem. Res **41**, 699 (2008).
[14] L. M. Huang, H. Z. Lin, T. C. Wen, A. Gopalan, Electrochim. Acta **52**, 1058 (2006).
[15] J. Wang, B. L. Deng, H. Chen, X. R. Wang, J. Z. Zheng, Environ. Sci. Technol **43**, 5223 (2009).
[16] S. K. Li, X. F. Lu, X. Li, Y. P. Xue, C. C. Zhang, J. Y. Lei, C. Wang, J. Colloid Interface Sci **378**, 30 (2012).
[17] S. Majid, M. E. Rhazi, A. Amine, A. Curulli, G. Palleschi, Microchim. Acta **143**, 195 (2003).
[18] L. Zhang, L. Chai, J. Liu, H. Wang, W. Yu, P. Sang, Langmuir **27**, 13729 (2011).
[19] Y. Chen, X. Zhang, P. Yu, Y. Ma, Chem. Commun **30**, 4527 (2009)
[20] X. G. Li, M. R. Huang, S. X. Li, Acta Mater **52**, 5363 (2004).